Self-affine fractality in π^+p and K^+p collisions at 250 GeV/c

EHS/NA22 Collaboration

N.M. Agababyan[8], M.R. Atayan[8], M. Charlet[4,a], J. Czyżewski[4,b], E.A. De Wolf[1,c], K. Dziunikowska[2,d], A.M.F. Endler[5], Z.Sh. Garutchava[6], H.R. Gulkanyan[8], R.Sh. Hakobyan[8], J.K. Karamyan[8], D. Kisielewska[2,d], W. Kittel[4], L.S. Liu[7], S.S. Mehrabyan[8], Z.V. Metreveli[6], K. Olkiewicz[2,d], F.K. Rizatdinova[3], E.K. Shabalina[3], L.N. Smirnova[3], M.D. Tabidze[6], L.A. Tikhonova[3], A.V. Tkabladze[6], A.G. Tomaradze[6,e], F. Verbeure[1], Y.F. Wu[4,f], S.A. Zotkin[3]

[1] Department of Physics, Universitaire Instelling Antwerpen, B-2610 Wilrijk, Belgium
[2] Institute of Physics and Nuclear Techniques of Academy of Mining and Metallurgy and Institute of Nuclear Physics, PL-30055 Krakow, Poland
[3] Nuclear Physics Institute, Moscow State University, RU-119899 Moscow, Russia
[4] High Energy Physics Institute Nijmegen (HEFIN), University of Nijmegen/NIKHEF, NL-6525 ED Nijmegen, The Netherlands
[5] Centro Brasileiro de Pesquisas Fisicas, BR-22290 Rio de Janeiro, Brazil
[6] Institute for High Energy Physics of Tbilisi State University, GE-380086 Tbilisi, Georgia
[7] Institute of Particle Physics, Hua-Zhong Normal University, Wuhan 430070, China
[8] Institute of Physics, AM-375036 Yerevan, Armenia

Abstract: Taking into account the anisotropy of phase space in multiparticle production, a self-affine analysis of factorial moments was carried out on the NA22 data for π^+p and K^+p collisions at 250 GeV/c. Within the transverse plane, the Hurst exponents measuring the anisotropy are consistent with unit value (i.e. no anisotropy). They are, however, only half that value when the longitudinal direction is compared to the transverse ones. Fractality, indeed, turns out to be self-affine rather than self-similar in multiparticle production. In three-dimensional phase space, power-law scaling is observed to be better realized in self-affine than in self-similar analysis.

---

[a] EC guest scientist, now at DESY, Hamburg
[b] KUN Fellow from the Jagellonian University and fellow of the Polish Science Foundation (FNP) scholarship for the year 1996, Krakow
[c] Onderzoeksleider NFWO, Belgium
[d] Supported by the Polish State Committee for Scientific Research
[e] Now at UIA, Wilrijk, Belgium
[f] KNAW visitor from Hua-Zhong Normal University, Wuhan, China

1 Introduction

The suggestion that normalized factorial moments $F_q(\delta y)$ of particle-multiplicity distributions in ever smaller phase-space intervals δy, may show power-law behavior [1]

$$F_q(\delta y) \propto (\delta y)^{-\phi_q} \quad , \qquad (\delta y \to 0) \tag{1}$$

has spurred a vigorous experimental search for linear dependence of $\ln F_q$ on $-\ln \delta y$ [2]. Analogous to a similar behavior at the onset of turbulence, such a dependence is referred to as "intermittency". Power-law scaling is typical for fractals [3], i.e., for self-similar objects of non-integer dimension. The powers ϕ_q are related to the anomalous dimensions $d_q = \phi_q/(q-1)$ measuring the fractality of a system [4]. In general, however, only approximate scaling has been observed in the experimental data.

When comparing log-log plots for one phase-space dimension, one notices that the $\ln F_q$ saturate at small δy. This can be explained as a projection effect of a three-dimensional phenomenon [5]. In three-dimensional analysis, however, the power law also does not hold exactly in all data. In NA22, for example, the 3D data are seen to even bend upward [6].

A deviation from exact scaling can be expected from an anisotropy of occupied phase-space. To account for such an anisotropy, Wu and Liu have suggested [7] that the scaling property should be different in longitudinal and transverse directions and the local multiplicity fluctuations are *self-affine* rather than *self-similar*. If that is the case, the anomalous scaling of factorial moments can be observed to be retained exactly, only under a self-affine analysis, where the shrinking ratio is allowed to be different in different directions. In a self-similar analysis, in contrast, all directions are forced to have an identical shrinking ratio. It should be remembered, however, that the scaling law is expected to be distorted in full phase space due to correlations imposed by momentum conservation.

The experimental data sample is described in Sect. 2. The method of self-affine analysis is briefly summarized in Sect. 3. The results of the self-similar analysis are shown in Sect. 4. After reducing the influence of momentum conservation in the full region, so-called Hurst exponents are obtained by fitting one-dimensional factorial moments as shown in Sect. 5. In Sect. 6, the results from the self-affine analysis compared to those from the self-similar analysis are given. Conclusions are summarized in Sect. 7.

2 The data sample

In the CERN experiment NA22, the European Hybrid Spectrometer (EHS) was equipped with the Rapid Cycling Bubble Chamber (RCBC) as an active target and exposed to a 250GeV/c tagged, positive, meson enriched beam. In data taking, a minimum bias interaction trigger was used. The details of spectrometer and trigger can be found in [8,9].

Charged particle tracks are reconstructed from hits in the wire- and drift-chambers of the two-lever-arm magnetic spectrometer and from measurements in the bubble chamber. The momentum resolution varies from 1-2% for tracks reconstructed in RCBC, to 1-2.5% for tracks reconstructed in the first lever arm and is 1.5% for tracks reconstructed in the full spectrometer.

Events are accepted for the analysis when the measured and reconstructed charge multiplicity are the same, charge balance is satisfied, no electron is detected among the secondary tracks and the number of badly reconstructed (and therefore rejected) tracks is 0. The loss

of events during measurement and reconstruction is corrected for by applying a multiplicity-dependent event weight normalized to the topological cross sections given in [9]. Elastic events are excluded. Furthermore, an event is called single-diffractive and excluded from the sample if the total charge multiplicity is smaller than 8 and at least one of the positive tracks has a Feynman variable $|x_{\rm F}| > 0.88$. After these cuts, the inelastic, non-single-diffractive sample consists of 59 200 π^+p and $\rm K^+p$ events.

For laboratory-momenta $p_{\rm LAB} < 0.7{\rm GeV}/c$, the range in the bubble chamber and/or the change of track curvature is used for proton identification. In addition, a visual ionization scan is used for $p_{\rm LAB} < 1.2{\rm GeV}/c$ on the full $\rm K^+p$ and on 62% of the π^+p sample. Positive particles with $p_{\rm LAB} > 150{\rm GeV}/c$ are given the identity of the beam particle. Other particles with momenta $p_{\rm LAB} > 1.2$ GeV/c are not identified in the present analysis and are treated as pions.

In spite of the electron rejection mentioned above, residual Dalitz decay and γ conversion near the vertex still contribute to the two-particle correlations. Their influence on our results has been investigated in detail in [10].

3 The method

In the language of self-affine analysis in three-dimensional phase space (here denoted as p_a, p_b, p_c), only under the self-affine transformation $\delta p_a \to \delta p_a/\lambda_a$, $\delta p_b \to \delta p_b/\lambda_b$, $\delta p_c \to \delta p_c/\lambda_c$ with non-identical shrinking ratios λ_a, λ_b and λ_c, are the factorial moments expected to have the well-defined scaling property

$$F_q(\delta p_a, \delta p_b, \delta p_c) = \lambda_a^{\phi_q^{(a)}} \lambda_b^{\phi_q^{(b)}} \lambda_c^{\phi_q^{(c)}} F_q(\lambda_a \delta p_a, \lambda_b \delta p_b, \lambda_c \delta p_c). \tag{2}$$

The shrinking ratios $\lambda_a, \lambda_b, \lambda_c$ are characterized by the so-called roughness or Hurst exponents [11]

$$H_{ij} = \frac{\ln \lambda_i}{\ln \lambda_j}, \qquad (i,j = a,b \quad \text{or} \quad a,c \quad \text{or} \quad b,c \quad), \tag{3}$$

with

$$\lambda_i \le \lambda_j, \qquad 0 \le H_{ij} \le 1, \tag{4}$$

describing the anisotropy of the system under study. For $H_{ij} = 0$, $\lambda_i = 1$, the scaling property does not exist in direction i, only in direction j. For $H_{ij} = 1$, the self-affine transformation reduces to a self-similar one, meaning that the system is isotropic in these two directions. For $0 < H_{ij} < 1$, non-trivial self-affine fractality exists in the (i,j) plane, i.e, the fluctuation is anisotropic in that plane.

The Hurst exponents can be deduced from the data by fitting three one-dimensional second-order factorial-moment saturation curves [5]

$$F_2^{(i)}(M_i) = \alpha_i - \beta_i M_i^{-\gamma_i}, \qquad (i = a,b,c) \tag{5}$$

where $M_i = \Delta p_i/\delta p_i$ is the number of sub-divisions in direction i, Δp_i and δp_i are the initial and final interval size in direction i, respectively, and α_i, β_i and γ_i are three fit parameters. The Hurst exponents are determined from the parameter γ_i as

$$H_{ij} = \frac{1+\gamma_j}{1+\gamma_i}, \qquad (i,j = a,b \quad \text{or} \quad a,c \quad \text{or} \quad b,c). \tag{6}$$

With these Hurst exponents, a self-affine analysis can be executed according to (2). If self-affine fluctuations of multiplicity do exist in multiparticle production, exact scaling should be observed in three-dimensional phase space.

A scaling function similar to (2) for two variables has also been suggested by J. Wosiek [12] as a requirement for hyperscaling from a formal analogy with statistical physics.

4 Self-similar analysis

The results of a *self-similar* analysis in 1-, 2- and 3-dimensional phase space are presented in Fig. 1. The initial intervals for the three phase-space variables, rapidity y, azimuthal angle φ and transverse momentum p_{t}, are defined as:

$$-2 < y < 2$$

$$0 < \varphi \leq 2\pi$$

$$0.001 < p_{\mathrm{t}} < 10 \text{ GeV}/c.$$

To avoid trivial effects due to lack of translational invariance, all variables are transformed to the corresponding cumulative variables by the Ochs method [13]. The experimental resolution in y, φ and p_{t} has been studied in detail in [10]. The limited available statistics, rather than the experimental resolution, sets the limit on the smallest bin size to be used in the analysis.

In one-dimensional projection, the partitioning $M = 1, 2, \ldots 40$ is used for all three variables. In two-dimensional projection, the partitioning in each direction is $M = 1, 2, \ldots 20$, so that for the area it is $M_2 = 1^2, 2^2, \ldots 20^2$. In the three-dimensional case, $M = 1, 2, \ldots 15$ is used for each direction, so that $M_3 = 1^3, 2^3, \ldots 15^3$ for a three-dimensional box.

In the 1-D analysis (first column of Fig. 1), F_2 saturates at three different values when using y, p_{t} and φ, respectively. In the case of y, F_2 increases rapidly with increasing $\ln M$ at small M and reaches a saturation value which is the highest of the three. The trend is followed for the case of p_{t}, but at lower values of F_2. When using φ, on the other hand, F_2 increases with increasing $\ln M$ only above an initial decrease.

From the 2-D analysis (second column of Fig. 1) in the (y, p_{t}) plane, we observe an onset for a saturation at medium $\ln M$, followed by an upward bending at large $\ln M$. An upward bending is observed in the (y, φ) plane. In the $(p_{\mathrm{t}}, \varphi)$ plane, a decrease at low $\ln M$ is followed by an upward bending.

In the 3-D analysis, $\ln F_q$ is bending upward for all orders of q.

5 Hurst exponents for higher-dimensional phase space

Momentum conservation by itself causes a correlation and can, therefore, distort the scaling behavior expected from the dynamics of particle production [14]. The influence of momentum conservation on the factorial moments is expected to be different in the various variables. The variable p_{t} contains only the absolute value of momentum in the transverse plane without any information on the direction. The influence of momentum conservation, therefore, is small for this case. For rapidity y, the influence of leading particles is reduced by the y-cut given above. Therefore, the influence of momentum conservation in y is not significant. For the variable φ, however, all directions in the transverse plane are included for $M = 1$, so that F_2

is dominated by transverse momentum compensation, which explains the decrease of $F_2(\varphi)$ with increasing $\ln M$ at low $\ln M$ as shown in Fig. 1.

After reducing the influence of momentum conservation by excluding low values of M, it is easy to obtain the Hurst exponents from the data by means of (5) and (6). The fit results obtained according to (5) are shown in Fig. 2 for all phase-space variables considered. The parameter values are given in Table 1. Accordingly, the Hurst exponents deduced from (6) are:

$$H_{yp_{\rm t}} = \frac{1.021}{2.14} = 0.48 \pm 0.06 \ ;$$
$$H_{y\varphi} = \frac{1.0139}{2.14} = 0.47 \pm 0.06 \ ;$$
$$H_{p_{\rm t}\varphi} = \frac{1.014}{1.0212} = 0.99 \pm 0.01 \ .$$

From these Hurst exponents, we, indeed, observe anisotropy ($H_{yj} \approx 0.5$) between longitudinal and transverse directions of multiparticle production, while there is an isotropy in the transverse plane ($H_{ij} \approx 1$ for i and j both in the transverse plane). This result means that fractality in multiparticle production is self-affine rather than self-similar.

In order to show the independence of this conclusion of the particular set of variables being used, the same analysis has also been done with the set $(y, p_{\rm ty}, p_{\rm tz})$ instead of $(y, p_{\rm t}, \varphi)$. The corresponding results for the Hurst exponents are:

$$H_{yp_{\rm ty}} = \frac{1.0121}{2.14} = 0.47 \pm 0.06 \ ;$$
$$H_{yp_{\rm tz}} = \frac{1.0041}{2.14} = 0.47 \pm 0.06 \ ;$$
$$H_{p_{\rm ty}p_{\rm tz}} = \frac{1.0041}{1.0121} = 0.99 \pm 0.01 \ .$$

They show that the rule $H_{yj} \approx 0.5$, $H_{ij} \approx 1$ for i and j denoting variables in the transverse plane also holds for the variable set $(y, p_{\rm ty}, p_{\rm tz})$.

6 Self-affine analysis

With the Hurst exponents obtained above, we can perform a self-affine analysis in three- and two-dimensional phase space. For convenience, we approximate the Hurst exponent for $(y, p_{\rm t})$ and (y, φ) by

$$H_{yj} = \frac{1}{2}, \qquad (j = p_{\rm t}, \varphi),$$

but use

$$H_{p_{\rm t}\varphi} = 1.$$

From (3), it follows that $\lambda_{p_{\rm t}} = \lambda_\varphi = \lambda_y^2$. For $p_{\rm t}$ and φ, we use a partitioning $M_y = 1, 2, 3, \ldots, 10$ and $M_{p_{\rm t}} = M_\varphi = 1, 4, 9, \ldots, 100$ in two-dimensional analysis, but $M_y = 1, 2, 3, \ldots, 7$ and $M_{p_{\rm t}} = M_\varphi = 1, 4, 9, \ldots, 49$ in three-dimensional analysis. The results of the three-dimensional self-affine analysis on F_2 are given by solid circles in Fig. 3. Those of

the corresponding self-similar analysis are repeated by open circles, for comparison. In order to show the quality of the scaling law, linear fits

$$\ln F_q = A + \phi_q \ln M_y \tag{7}$$

are compared to the data in Fig. 3. The fit results are given in Table 2. To reduce the influence of momentum conservation, the first point is not used in the fits.

Contributions to χ^2 as shown in the top part of Table 2 are only from the diagonal terms of the covariance matrix. In fact, the diagonal terms provide the main contribution, and the relative size of χ^2 for self-similar and self-affine analyses should not change dramatically by adding the contribution from non-diagonal terms that account for the correlation between points at different bin size. As is shown by comparing the results from fits to the unweighted sample, with and without considering the non-diagonal terms (two lower parts of Table 2), the fit results are retained better for the self-affine than for the self-similar analysis. A similar conclusion can be drawn from an inspection of Fig. 3, itself. While the self-similar analysis leads to an upward bending, this effect is absent in the self-affine analysis. Of course, higher statistics data would be needed to definitively prove this point.

Even though the errors in the self-affine analysis are large, the results shown in Fig. 3 support the expectation [7] that a 3-dimensional self-affine analysis would lead to the full increase of $\ln F_q$ with increasing $\ln M$ right from the beginning. On the other hand, in a self-similar analysis, the full increase would only be reached for large M, so that an upward bending would be observed. This upward bending is indeed present for the self-similar analysis. If future experiments can confirm the linear increase of the self-affine results with improved statistics, this would mean that the scaling law (1) is better observed in self-affine analysis than in self-similar analysis.

The two-dimensional self-affine projections are presented in Fig. 4. It can be seen that $\ln F_2$ increases smoothly with increasing $\ln M_y$ and the trends are similar for (y, p_t) and (y, φ) (neglecting the first point in (y, φ)), meaning that in a self-affine analysis, the influence of artificial projection effects is reduced with respect to that observed in self-similar analysis.

7 Conclusions

In this paper we present a self-affine analysis of factorial moments in three-, as well as in two-dimensional phase space, on the NA22 data for π^+p and K^+p collisions at 250 GeV/c. The results are compared with those from a corresponding self-similar analysis.

From fitting the factorial moments of the one-dimensional projections by the Ochs saturation formula (5), the Hurst exponents H_{ij} are derived for all combinations of phase-space variables used. The value of H_{ij} for a combination of rapidity y with a transverse direction is approximately equal to 0.5. We conclude, therefore, that fractality in multiparticle production is self-affine, rather than self-similar. In the transverse plane, H_{ij} stays approximately equal to 1.0 and, therefore, shows merely self-similar fluctuation within that particular plane. Such a behavior can be understood from the privileged role of the longitudinal axis in multihadron production and the symmetry within the plane transverse to this direction. This important point has been neglected in fluctuation analysis of multiparticle final states, so far.

Furthermore, the three-dimensional self-affine analysis shows a better scaling behavior than does the corresponding self-similar analysis. The two-dimensional self-affine projections with $H_{ij} = 0.5$, i.e., (y, p_t) and (y, φ) turn out to show a behavior more similar to each other than in the corresponding self-similar projections.

It would be interesting to see how the value of H_{ij} changes with the type of collision and with incident energy.

Acknowledgments

We are grateful to the III. Physikalisches Institut B, RWTH Aachen, Germany, the DESY-Institut für Hochenergiephysik, Berlin-Zeuthen, Germany, the Department of High Energy Physics, Helsinki University, Finland, the Institute for High Energy Physics, Protvino, Russia, and the University of Warsaw and Institute of Nuclear Problems, Warsaw, Poland, for early contributions to this experiment.Work is supported in part by Polish KBN grant no. 2 P03B 083 08 and by Polish-German Collaboration Foundation FWPN no. 1441/LN/94. This work is part of the research program of the "Stichting voor Fundamenteel Onderzoek der Materie (FOM)", which is financially supported by the "Nederlandse Organisatie voor Wetenschappelijk Onderzoek (NWO)". We further thank NWO for support of this project within the program for subsistence to the former Soviet Union (07-13-038). The work is also a part of the research project "Density Fluctuations in Multiparticle Production", supported by the National Commission of Science and Technology of China and the Koninklijke Nederlandse Akademie van Wetenschappen (KNAW). It is, furthermore, supported in part by the NNSF of China, the DYTF of the State Education Commission of China and the CGP for young scientists of Wuhan City.

REFERENCES

1. A. Białas and R. Peschanski: Nucl. Phys. B273 (1986) 703 and B308 (1988) 857.
2. See for example the review article: E. A. De Wolf, I. M. Dremin and W. Kittel: Scaling Laws for Density Correlations and Fluctuations in Multiparticle Dynamics, Nijmegen Preprint HEN-362 (1995), Phys. Report (1996), in press.
3. B. Mandelbrot: The Fractal Geometry of Nature (Freeman, NY, 1982).
4. P. Lipa and B. Buschbeck: Phys. Lett. B223 (1989) 465.
5. W. Ochs: Phys. Lett. B247 (1990) 101.
6. N. Agababyan et al., NA22 Coll.: Z. Phys. C59 (1993) 405 and Phys. Lett. B332 (1994) 458.
7. Wu Yuanfang and Liu Lianshou: Phys. Rev. Lett. 21 (1993) 3197.
8. M. Aguilar-Benitez et al.: Nucl. Instrum. Methods 205 (1983) 79.
9. M. Adamus et al., NA22 Coll.: Z. Phys. C32 (1986) 475.
10. F. P. M. Botterweck: Ph.D. Thesis, University of Nijmegen, 1992.
11. B. Mandelbrot in Dynamics of Fractal Surfaces, eds. E. Family and T. Vicsek (World Scientific, Singapore, 1991).
12. J. Wosiek: Proc. XXIV International Symposium on Multiparticle Dynamics, Vietri sul Mare (Italy) 1994, eds. A. Giovannini, S. Lupia and R. Ugoccioni (World Scientific, Singapore, 1995) p. 99.
13. W. Ochs: Z. Phys. C50 (1991) 339.
14. Liu Lianshou, Zhang Yang and Deng Yue: On the influence of momentum conservation upon the scaling behaviour of factorial moments in high energy multiparticle production, Wuhan preprint HZPP-9605 (1996), Z. Phys. C, in press.

Table 1. The parameter values obtained from a fit by (5).

variables	a	b	c	Omitting point(s)
y	1.336 ± 0.005	0.218 ± 0.042	1.140 ± 0.245	1
$p_{\rm t}$	1.534 ± 0.021	0.340 ± 0.021	0.021 ± 0.006	1
φ	1.497 ± 0.019	0.420 ± 0.019	0.014 ± 0.005	$1-3$

Table 2. The parameter values obtained from a fit by (7).

method	without bin-size correlation		
	A	ϕ_2	χ^2/NDF
weighted self-affine	-0.04 ± 0.03	0.32 ± 0.03	7/4
weighted self-similar	0.11 ± 0.01	0.12 ± 0.01	9/4
method	without bin-size correlation		
	A	ϕ_2	χ^2/NDF
unweighted self-affine	-0.08 ± 0.02	0.33 ± 0.03	12/4
unweighted self-similar	0.09 ± 0.01	0.10 ± 0.01	20/4
method	with bin-size correlation		
	A	ϕ_2	χ^2/NDF
unweighted self-affine	-0.08 ± 0.02	0.34 ± 0.02	14/4
unweighted self-similar	0.10 ± 0.01	0.10 ± 0.01	32/4

FIGURE CAPTIONS

Fig. 1 Self-similar analysis of F_q in the set of variables (y, p_t, φ) in one, two, and three dimensions, as indicated.

Fig. 2 Saturation curves for F_2 in the three one-dimensional variables indicated. The curves are fits by (5) after omission of the first point (first 3 points in the case of $F_2(\varphi)$).

Fig. 3 Comparison of the three-dimensional self-affine and self-similar analyses.

Fig. 4 Comparison of the two-dimensional projections of self-affine and self-similar analyses.

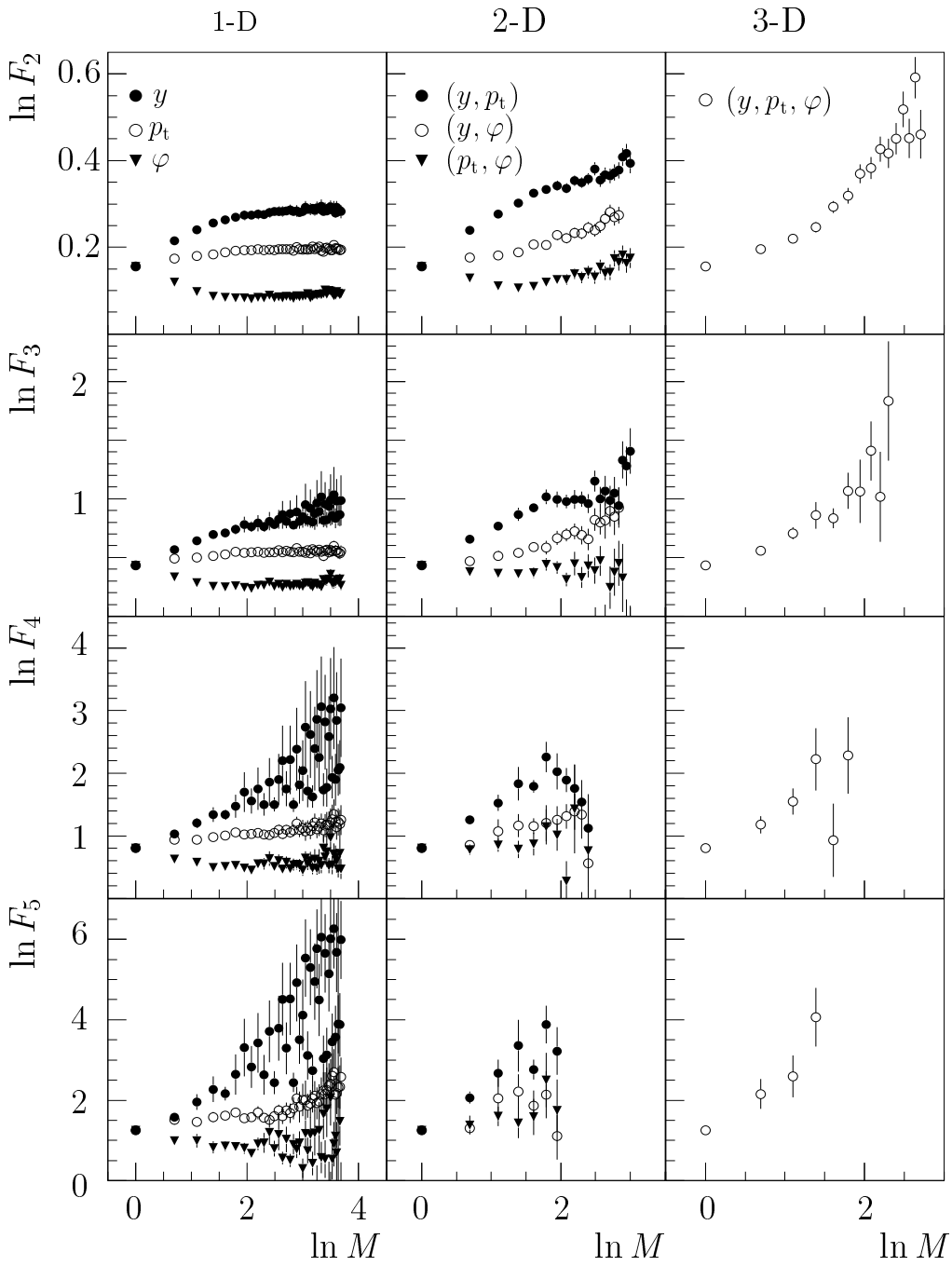
1-D
2-D
3-D
ln F_2
ln F_3
ln F_4
ln F_5
y
p_t
φ
(y, p_t)
(y, φ)
(p_t, φ)
(y, p_t, φ)
ln M

Fig. 1

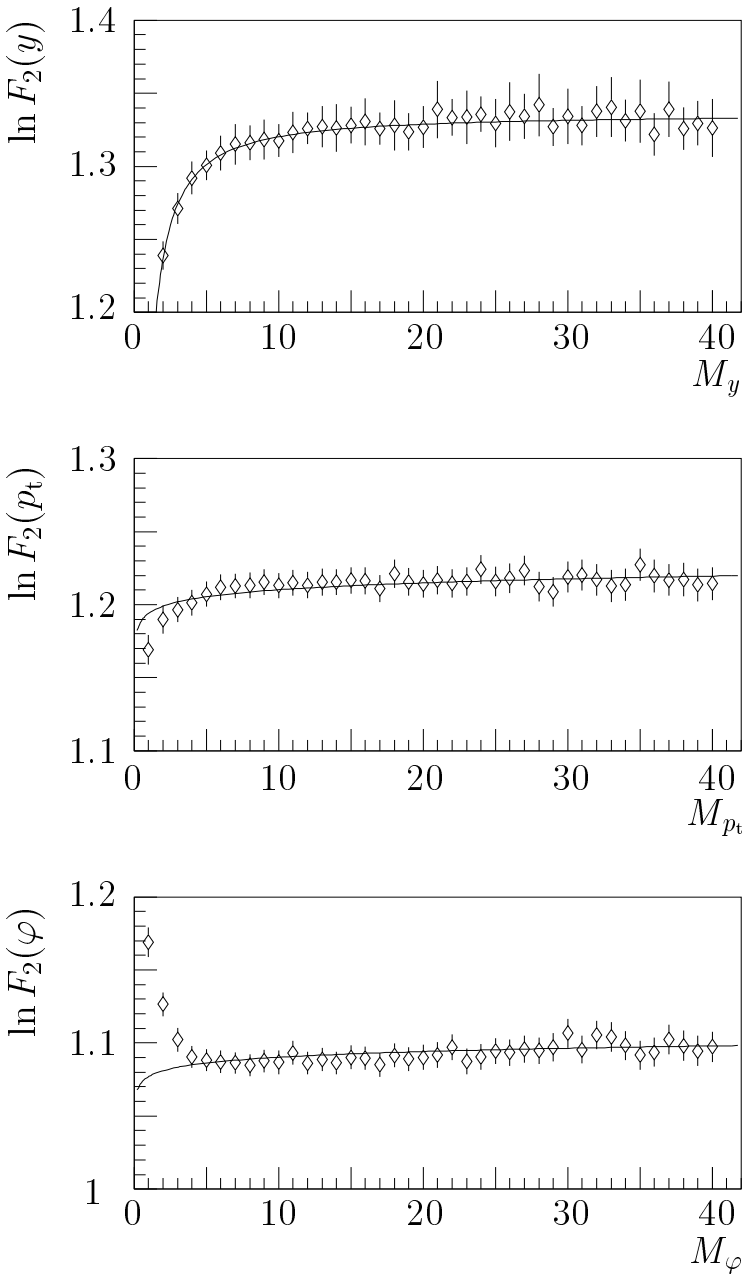
$\ln F_2(y)$
1.4
1.3
1.2
0
10
20
30
40
M_y
$\ln F_2(p_t)$
1.3
1.2
1.1
0
10
20
30
40
M_{p_t}
$\ln F_2(\varphi)$
1.2
1.1
1
0
10
20
30
40
M_φ

Fig. 2

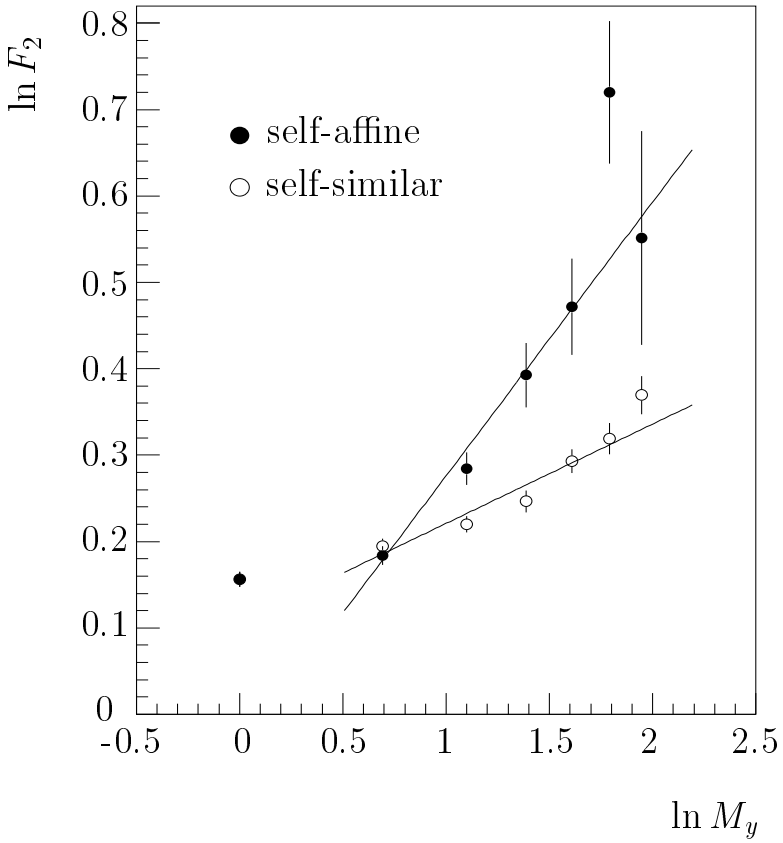
0.8
0.7
0.6
0.5
0.4
0.3
0.2
0.1
0
-0.5
0
0.5
1
1.5
2
2.5
ln F_2
ln M_y
self-affine
self-similar

Fig. 3

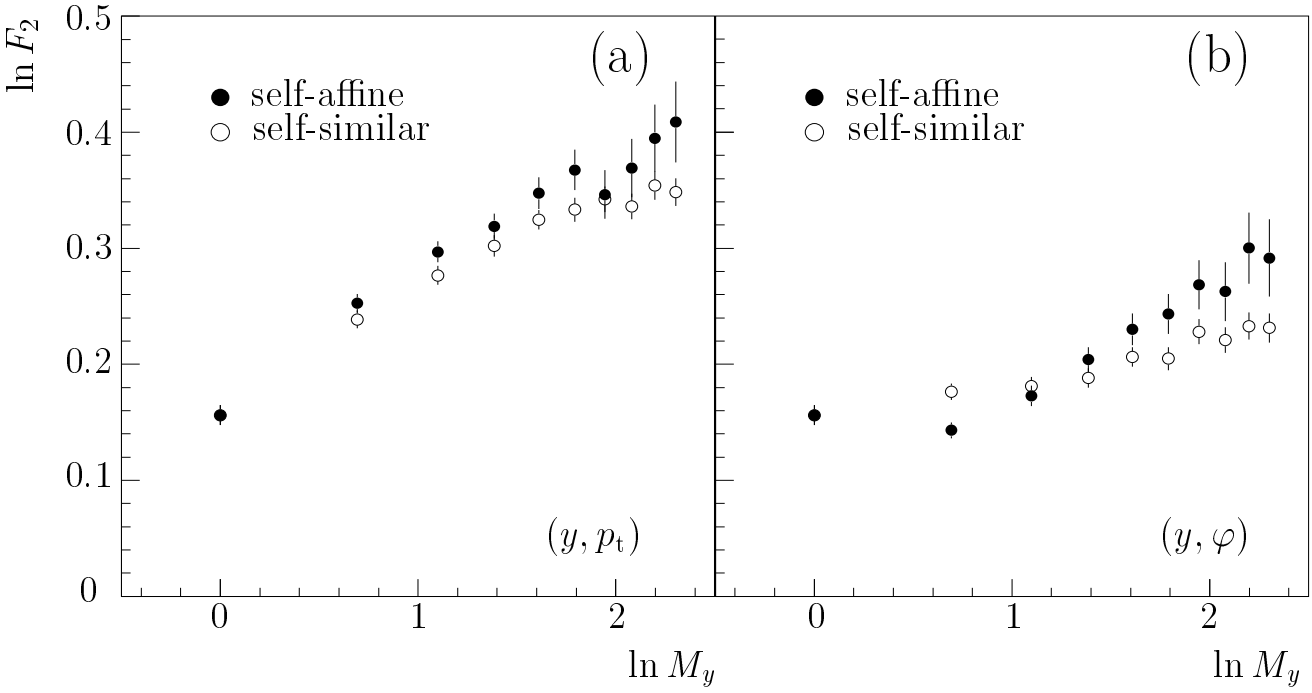
ln F_2
0.5
0.4
0.3
0.2
0.1
0
(a)
self-affine
self-similar
(y, p_t)
(b)
self-affine
self-similar
(y, φ)
0
1
2
ln M_y
0
1
2
ln M_y

Fig. 4